Applied Acoustics 124 (2017) 20–29

Contents lists available at ScienceDirect

Applied Acoustics

journal homepage: www.elsevier.com/locate/apacoust

Loudspeaker FEM modelling: Characterisation of critical aspects in acoustic impedance measure through electrical impedance

Francesco Bianco [a,b], Luca Teti [b], Gaetano Licitra [c,*], Mauro Cerchiai [d]

[a] IPCF-CNR, UOS di Pisa, Via G. Moruzzi 1, Pisa, Italy
[b] iPOOL srl, Ripa Castel Traetti 1, Pistoia, Italy
[c] ARPAT, Area Vasta Costa, Via Marradi 114, 57126 Livorno, Italy
[d] ARPAT, Area Vasta Costa, Settore Agenti Fisici, Via Vittorio Veneto 27, 56127 Pisa, Italy

ARTICLE INFO

Article history:
Received 3 August 2016
Received in revised form 23 December 2016
Accepted 6 March 2017
Available online 2 April 2017

Keywords:
Loudspeaker
FEM
Acoustic impedance
Acoustic absorption

ABSTRACT

A loudspeaker can be seen as a device coupling different acoustic, mechanic and electric systems by a series of impedance adaptations. A simple model can thus allow the determination of the acoustic impedance seen by the speaker membrane from measuring the electric impedance of the device. Given a certain number of assumption on mechanical modes and on the strictly electric components, this approach in principle is valid through a wide frequency range. Applying this method with a loudspeaker or a similar device allows to perform acoustic impedance measurements, as shown by Ahadi and Bakhtiar in a previous work. Unfortunately, when trying to apply straightforwardly this method, many difficulties arise. In this paper, using a FEM simulation of a loudspeaker in specific mounting conditions, critical aspects are highlighted to improve the range of application of the measurement technique. Moreover, the role of the speaker' s geometry is separately analysed and possible methods to overcome the limitations of the measuring method are provided. Further developments will be necessary to deal with time varying and nonlinear properties of the speaker.

1. Introduction

The behaviour of a sound plane wave travelling through a medium can be completely described by its wave number, the amplitude and the characteristic acoustic impedance of the material, defined as the ratio between the wave pressure and fluid velocity. When another medium is encountered, a part of the wave is transmitted and a part is reflected, according to the differences between the media impedances: hence the acoustic impedance of a separation surface can then be defined and linked to the wave reflection and energy absorption. Having knowledge on the acoustic impedance is then of great importance to accurately predict a medium' s acoustical behaviour, such as the acoustical absorption. There are many different measuring techniques that allow the evaluation of the acoustic impedance as a function of the frequency: the impedance tube in its implementations (in laboratory [1,2] and in situ [3]) and the free field signal subtraction techniques as Adrienne [4,5] are possible examples. These methods are generally based on a microphonic measurement of the pressure wave and its subsequent analysis, however more advanced sensors as the p-u probe can be used to achieve a direct evaluation of the impedance [6], being able to measure both the pressure and the particle velocity of the travelling wave. Some common issues of the aforementioned methods can be pointed out: first, it is required an accurate knowledge on the frequency response of the measuring chain and secondly a good calibration on the whole frequency range must be attained. Such requests often translate into expensive or complex instrumentation that must also be maintained during time with calibration costs. A different and simpler approach to this problem arises from the observation that a loudspeaker is indeed a series of coupled electrical, mechanical and acoustical systems. The electromagnetic induction on a voltage driven spire allows the feedback between the electrical parts and the mechanical ones, which includes the acoustical load on the speaker membrane. The electric impedance of this system is then dependent on its mechanical reactance, resistance and compliance, besides on the acoustic impedance over the membrane. On the basis of these assumptions, the loudspeaker can be seen as both source and probe of an acoustic signal. This method could in principle allow to reduce initial and maintenance expenses with a simpler measurement chain, leading for example to portable instruments for in situ acoustical absorption measurement. The work of Ahadi and Bakhtiar [7] showed

* Corresponding author.
E-mail addresses: sephir@gmail.com (F. Bianco), teti.luca@gmail.com (L. Teti), g.licitra@arpat.toscana.it (G. Licitra), m.cerchiai@arpat.toscana.it (M. Cerchiai).

http://dx.doi.org/10.1016/j.apacoust.2017.03.005
0003-682X/

the experimental feasibility of measuring the acoustical impedance of a closed duct from an electrical impedance measure. The speaker' s mechanical impedance is considered as an unknown quantity that has a piecewise linear behaviour as a function of frequency: a linear system is then solved for each assumed frequency step, when a known acoustical load is imposed on the speaker. The characterised speaker can then be used to extract unknown acoustic loads from its electric impedance measures. In this work the theory underlying the latter measuring technique is examined in depth and a FEM modelling (Comsol Multiphysics) is used to correctly evaluate limitations and critical aspects of the method. The advantages of verifying the theory using a FEM model are the following: more general results can be obtained, and the influence of every physical interaction and element of the problem can be evaluated, including the geometry and the materials of the system. Thus, no assumptions on the functional form of the speaker mechanical impedance are required.

2. Basic model

It is useful to describe the technique starting from a simple equivalent circuit model for a loudspeaker, following the approach described by Beranek [8]. The speaker is treated as an electrical circuit composed by a resistance, an inductance and a load given by electromechanical transduction that couples the mechanical part. The latter is, at low enough frequencies, a dampened spring-mass system with an added acoustic impedance load put in parallel. By Ohm' s law, the current I flowing in the circuit is defined as

$$I = \frac{V_0}{Z_{el}} \tag{1}$$

where V_0 is the applied electric potential and Z_{el} is the total electrical impedance. Assuming one-dimentional motion and defining u as the mechanical parts velocity and Z_b the wire impedance, the current I can be written as

$$I = \frac{V}{Z_b} = \frac{V_0 - Blu}{Z_b} \tag{2}$$

where Bl, also known as the force factor, is the product of the magnetic induction B and the spire of length l, V is the total electrical potential, defined by the difference between V_0 and the induced electromotive potential Blu.

The total force F_{tot} acting on the mechanical part is given by Lorentz law as

$$F_{tot} = BlI = Bl\frac{V_0 - Blu}{Z_b} \tag{3}$$

and it can also be written as

$$F_{tot} = uZ_{tot} = u(Z_m + Z_{ac}A_{sp}) \tag{4}$$

where Z_m is the speaker' s mechanical impedance and A_{sp} is the surface of the speaker' s membrane: the acoustical impedance Z_{ac} is expressed here as the ratio between pressure and local particle speed, therefore it is necessary to multiply it by the area of the speaker. It is important to point out that close to the membrane the mechanical and fluid velocities have the same value.

Finally using previous equations, the total electrical impedance Z_{el} can be written as

$$Z_{el} = Z_b + \frac{(Bl)^2}{Z_m + Z_{ac} \cdot A_{sp}} \tag{5}$$

which is the basic loudspeaker equation.

It must be noted that in general the acoustic impedance acting on a speaker' s membrane has a dependence on the position. The surface pressure can assume different values depending on the geometry of the generated acoustical wave. Surface stress should be expected, while strain is greatly reduced by the request of uniform velocity (or piston-like motion). With this constraint the surface integral of the acoustical impedance and the ratio of the total applied acoustical force and surface velocity have the same value: $\int Z_{ac}dS = \int P dS/v$.

When the coil movement is blocked, there is no electromotive force Blu induced by the mechanical circuit: the electrical impedance becomes then equal to Z_b alone, that is therefore also known as blocked coil impedance. This can also be seen from Eq. (5), in fact if u tends to zero the mechanical impedance grows to infinity, being defined as a P-u ratio, allowing to eliminate the equation' s rightmost term.

Observing that the loudspeaker is essentially a metallic coil linked to a moving dampened spring-mass system, it' s possible to express, as a first order approximation, the blocked coil impedance and the mechanical impedance as

$$Z_b = R_e + i\omega L_e \tag{6}$$

where R_e is the electrical resistance and L_e the inductance

$$Z_m = R_m + i\omega M_m + \frac{1}{i\omega C_m} \tag{7}$$

with M_m as the total moving mass, C_m the spring compliance and R_m the mechanical resistance linked to the viscous dispersion.

Eq. (5) describes a lumped mechanical model for the speaker, valid in principle when the wavelength is significantly greater than the largest size of its elements.

2.1. Model limitations

Some difficulties arise when trying to apply this simple model to a wide frequency range. Obviously, from a mechanical point of view, it is well known that any surface can show spatial modes when the stimulus' frequency rises. Then Eq. (5) is no longer valid nor can completely define the mechanical system described. In this work the correctness of Eq. (5) is assumed as well as simple plane motion for the membrane on a wide frequency range. An exact limit of the applicability of Eq. (5) cannot be described without taking into account every detail in the speaker' s membrane construction and placing, however it is reasonable to consider an upper frequency limit from a comparison between the wavelength and the membrane geometry. No stationary mode can appear for half wavelength greater than a circular surface diameter Ø, so an approximate criteria to select a frequency range f can be$f < c/(2Ø)$, where c is the speed of sound. Above this frequency value, it is necessary to take into account the system' s exact geometry and its mass and elasticity space distribution.

Nonlinear behaviour of the loudspeaker can also alter the results from the electrical impedance measurement. Klippel [9,10] showed that the blocked coil impedance can be dependent on the mean membrane displacement. In the full working range of displacement, elastic components do not alter significantly their Young modulus, but a small nonlinearity on the mechanical dissipation R_m can be observed. The two mentioned effects are significant only for high values of membrane displacement, which are not considered in the cases under examination.

Moreover, the acoustical part poses at least two main issues. The first is that the acoustical load is present on both the sides of the speaker membrane, even if it can be considered negligible when the front load is high as in an impedance tube device configuration. The second is the local nature of the acoustical impedance acting near the membrane' s surface extracted by the means of Eq. (5). Information carried by the wave from distant space regions can be greatly influenced by local geometry. A typical case

displaying these phenomena is the speaker mounting in the impedance tube and it will be discussed in detail in Section 5.

As a rule of thumb, the cone shape and its composition are very influential on the validity of Eq. (5). While it is difficult to correctly have knowledge on the materials involved in a loudspeaker' s membrane construction, it is fairly easy to define its geometry and this is the focus of the next sections of this work.

Lastly, regarding the electrical part of the circuit, the resistive and inductive terms of the blocked coil impedance Z_b show a frequency depending behaviour, which is addressed in further sections. There are also circuital models like the one proposed by Leach [11] or empirical ones such as Wright's [12] that deal with the issue. On the contrary, the approach proposed by Ahadi and Bakhtiar does not take into account this effect.

Given a specific set of electrical and acoustical impedance, Eq. (5) then forces a relation between the blocked coil impedance and the speaker mechanical one. Therefore the latter cannot be derived without using the correct Z_b frequency dependence. Other limitations are related with time varying properties caused by fatigue, aging, climate and coil orientation towards the gravitational pull. The application of the proposed method should take into account also these time constraints, limiting its validity to devices unaffected by aging and in unchanged position relatively to the system characterisation.

3. FEM model

To simplify the approach, the loudspeaker is represented in a 2D axial-symmetric environment as the rotation of its section. Despite of losing complete spatial information on the membrane behaviour, the computational cost is greatly reduced. Fig. 1 is an example of a simulated geometry, where different parts of the speaker can clearly be seen. The FEM model solution is divided in three steps, according to a known loudspeaker FEM modelling [13]. Initially the flux of the magnet (the cylindrical element in the right side of Fig. 1, in red in the online version of the paper) through the coil (in the bottom part of the cone) is calculated, acquiring in this way the force factor. The result is then used to obtain the blocked coil impedance as a function of the frequency. By applying a harmonic voltage $V_0 \exp(i\omega t)$ to the blocked system and knowing the spire, magnet and ferromagnetic core (the casing of the magnet) characteristics, the "blocked" current I_b is calculated. Z_b is then simply the ratio between the imposed voltage modulus V_0 and the calculated current.

As known, the effects leading to the frequency dependence of Z_b are mainly linked to induced currents that can exist on the surface and for a skin depth in the volumes of the conductive elements [11,12]. It' s important to have enough spatial resolution on the mesh for those elements in proximity of the surfaces. Once computed Z_b, it is possible to solve the last step of the simulation.

A further simplification can be introduced: as in Fig. 1 there is no explicit representation of the speaker' s elastic parts as the spider and the suspension, applying a lumped parameters approach. Their effect is applied directly to the moving parts, by imposing on them a load of the compliance and reactance term of Eq. (5), besides the electro-mechanical load induced by the applied voltage on the coil. This approach allows to neglect the study of correct material properties for the elastic parts, nonetheless it is important to notice that is equivalent to a complete speaker' s design, because in the considered frequency range the effect of the spatial modes due to geometry are negligible. When the elastic materials properties are chosen, Z_m can be derived by simply leaving out the acoustic load on the speaker' s surface, as it will be showed in following sections.

4. FEM results: blocked coil impedance

By computing the value of Z_b the resistive and inductive parts of the blocked coil impedance can be evaluated, respectively as $R_e = Re(Z_b)$ and $L_e = Im(Z_b)\,\omega^{-1}$. A frequency dependence results from the simulations of both terms.

This result, shown in Fig. 2, is coherent with models proposed in the audio engineering field [11,12] and shows the potentiality for FEM simulation to correctly address this issue in actual cases.

Although a work by Dodd et al. [9] has shown the possibility to achieve a good agreement between FEM and experimental value for Z_b, in this work it is carried out only a qualitative comparison, allowing to represent an actual system and evaluate its behaviour.

A measure is then performed on a 10 cm diameter loudspeaker, with a nominal resistance of 4 ω. The speaker is represented as an impedance in a simple voltage divider circuit, with a reference resistance of 5 ω at 1% precision. A broadband white noise signal is then fed to the system and the resulting voltage on the speaker is measured with a National NI 9234 board. The speaker is then blocked by mechanically fixing the central part transmitting motion to the membrane. In this way most of its emission is then stopped, even if some noise can still be heard.

Fig. 3 shows the results for the experimental measurement. Although the low frequency part of the resistance R_e has a slightly different behaviour, the FEM simulation shows a clear agreement with experimental data. It is possible to see that the values of both R_e and L_e change dramatically, especially in the low frequency

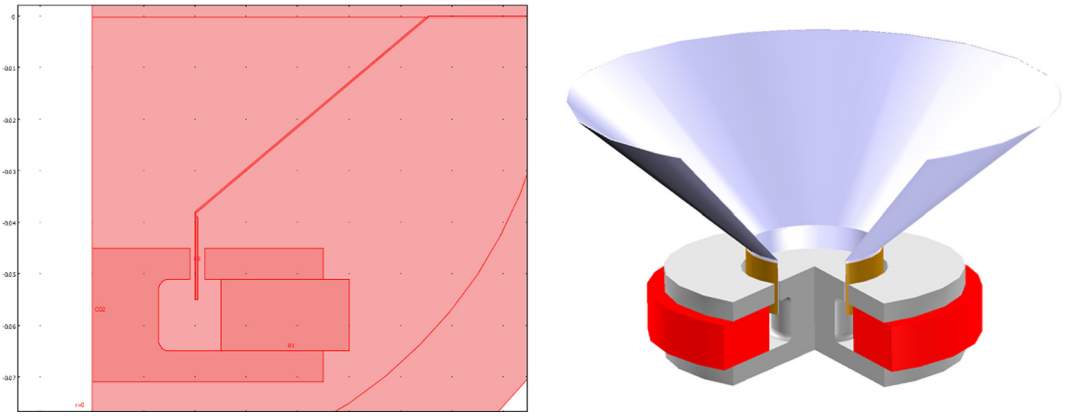

Fig. 1. Section of the model and its rotation along the axis is shown. A maximum diameter of 5 cm is used for the simulations, generally varying throat diameter and the height of the conical part.

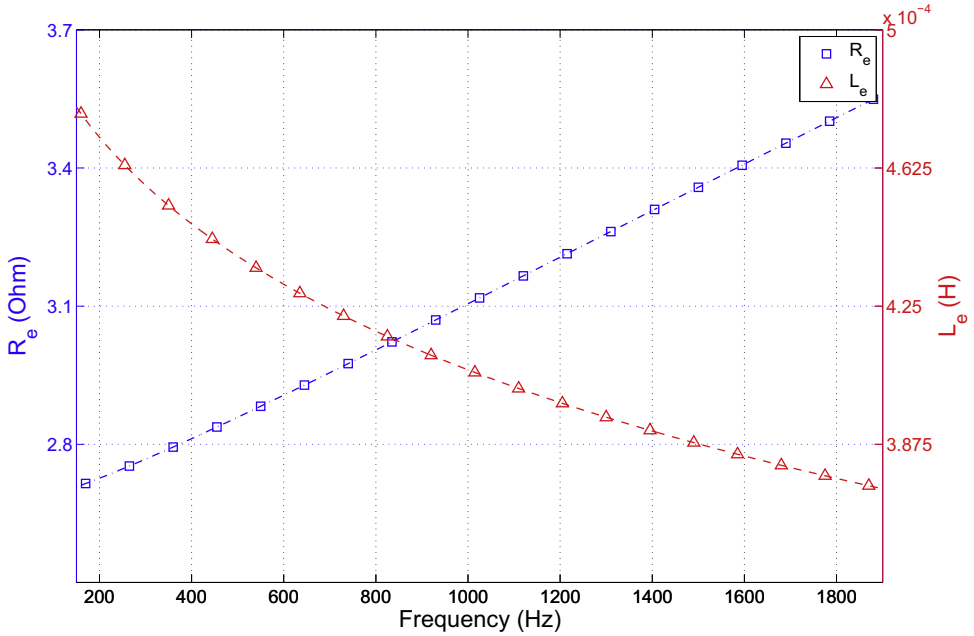

Fig. 2. FEM simulation results for the resistive R_e and inductive L_e parts of the blocked coil electrical impedance. [Referenced colours are shown in the online version of this paper.] (For interpretation of the references to colour in this figure legend, the reader is referred to the web version of this article.)

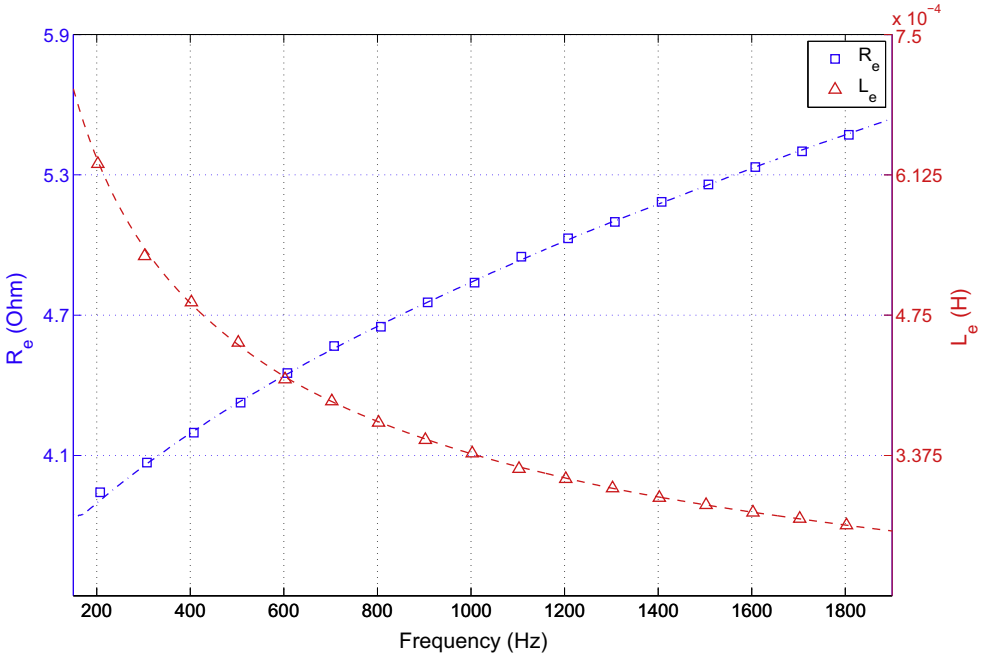

Fig. 3. Experimental results for the resistive R_e and inductive L_e parts of the blocked coil electrical impedance for the loudspeaker. [Referenced colours are shown in the online version of this paper.] (For interpretation of the references to colour in this figure legend, the reader is referred to the web version of this article.)

range, where the assumption of lumped mechanical elements is held true.

5. FEM results: mounting geometries

The case of a circular plate in an infinite baffle is firstly investigated to show the effects of surface modes on the extraction technique. Therefore, an evaluation on various more realistic speaker' s geometries is carried out, in conjunction to an impedance tube mounting. This condition allows not only to apply different acoustic loads on the speaker membrane, but also to evaluate the effect of the extraction technique on the acoustical energy absorption, in a condition easily replicable in laboratory.

5.1. Circular plate in infinite baffle

A simple circular thin plate with a diameter of 10 cm is placed in an infinite baffle mounting. The acoustical load is applied only on the plate' s upper surface and the simulation is repeated for different Young modulus values E_i for the membrane material, in order to evaluate the system' s behaviour when structural

resonances begin to appear. It is not applied any damping in order to enhance the resonance effect. Two cases are depicted here: $E_1 = 5 \cdot 10^{12}$ Pa and $E_2 = 2 \cdot 10^{18}$ Pa, respectively in Figs. 4, 5 and Figs. 6, 7. For the sake of simplicity, only the absolute values of the impedances, both the electrical and the acoustical ones, are represented in Figs. 4 and 6. They contain enough information to represent the described phenomenon. Figs. 5 and 7 show the comparison between both the real and the imaginary part of the extracted relative acoustical impedance and the theoretical one calculated for the presented setup according to the following equation [8]:

$$Z_{theo} = 1 - \frac{J_1(2k_0a)}{k_0a} + i\frac{H_1(2k_0a)}{k_0a} \tag{8}$$

where k_0 is the wavenumber, a is the plate radius and J_1 and H_1 are respectively first kind Bessel and Struve functions.

The E_1 Young modulus case is presenting a structural resonance on the speaker' s surface at approximately 1380 Hz. This is clearly reflected in the electrical impedance and it is interesting to notice that the relative acoustical one shows a similar peak at a lower frequency. This is a direct consequence on the inverse relation between Z_{ac} and $Z_{el} - Z_b$ arising from Eq. (5) and stresses the importance of a correct knowledge on the blocked coil impedance. The comparison in Fig. 5 shows complete disagreement between the theoretical and the extracted impedance except for very low frequencies, with a slightly better behaviour for the real part. It must be pointed out that Z_m has been extracted also for this case using the method described in Section 3: any information on the spatial localisation of the mode has been lost and Eq. (5) yields to an incorrect result. The E_2 Young modulus case is instead a perfect application of the extraction technique, in fact the plate behaves like a rigid piston for the whole considered frequency range and the calculated acoustical load is consistent with the theoretical prediction.

5.2. Realistic cone shape in an impedance tube

The tube mounting condition is useful to apply a wide range of surface impedances on the speaker. This can be simply achieved by imposing on the tube' s closed end a specific surface acoustical impedance, which value is derived from a model or taking advantage from an experimental measurement. In this study the second approach has been used, measuring in an impedance tube the surface impedance of a melamine foam and a porous pavement. Knowledge on sample surface acoustic impedance Z_{sur} allows to evaluate its acoustical energy absorption α, at least for a plane wave with orthogonal incidence:

$$\alpha = 1 - \left|\frac{Z_{sur} - Z_0}{Z_{sur} + Z_0}\right|^2 \tag{9}$$

where Z_0 is the characteristic acoustic impedance of air, 428.7 kg s^{-1} m^{-2} in standard conditions.

Three different cone shapes were implemented to further study geometry influence on the measurement, their characteristics are reported in Table 1 as depicted in Fig. 8. The different shapes lead to slightly different membrane masses, while the mechanical reactance and resistance are not modified, so a slight difference in the derived Z_m is to be expected. This should not be of any concern for the acoustical impedance calculation.

It' s well known that, in a closed tube configuration, the acoustical impedance is dependent on the distance from the backing,

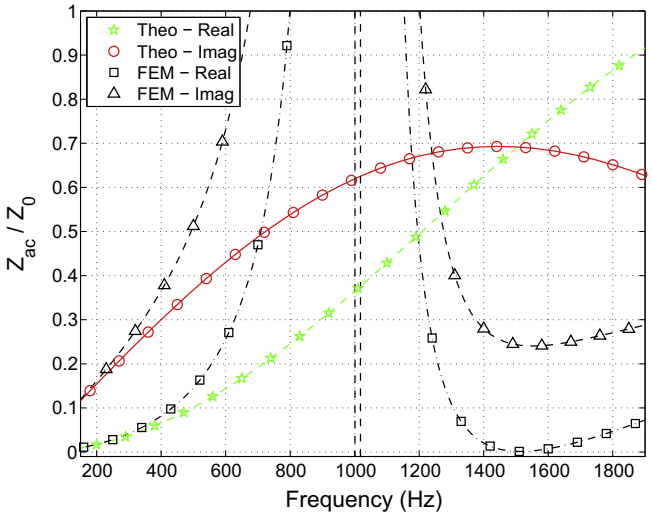

Fig. 5. Comparison between both the real (green solid line) and imaginary (red solid line) parts of the theoretical relative acoustical impedance Z_{theo} and both the real (black dotted line) and imaginary (black dashed line) parts of the extracted relative acoustical impedance Z_{ac}/Z_0. [Referenced colours are shown in the online version of this paper.] (For interpretation of the references to colour in this figure legend, the reader is referred to the web version of this article.)

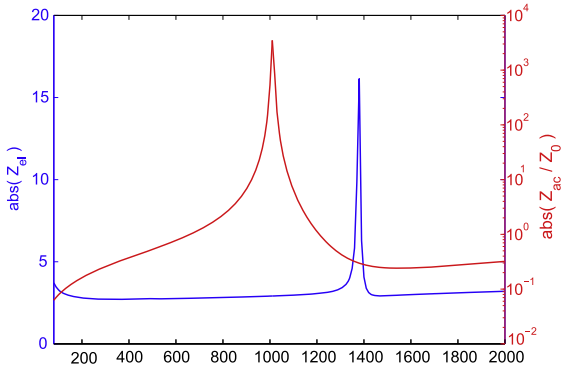

(a) Modulus of the electrical impedance Z_{el} and the extracted relative acoustical impedance Z_{ac}/Z_0.

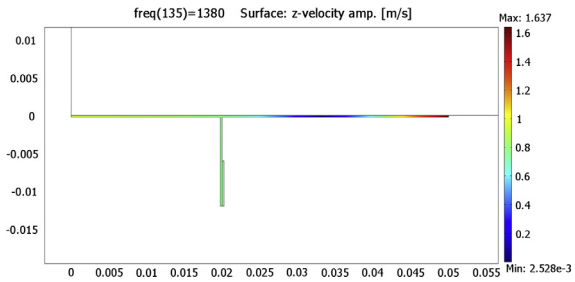

(b) Modulus of the velocity along the plate at the frequency 1380 Hz, where the electrical impedance shows a resonance.

Fig. 4. FEM results for Young modulus E_1: frequency behaviour and spatial velocity distribution at resonance.

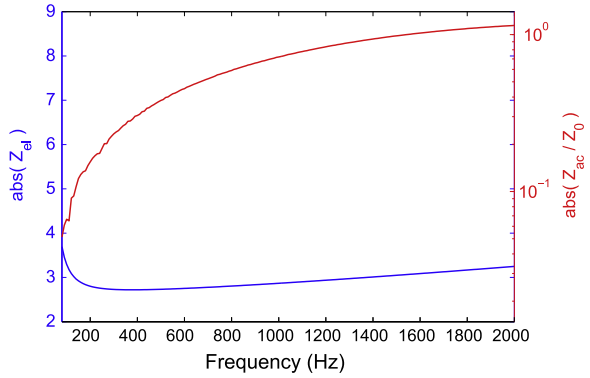

(a) Modulus of the electrical impedance Z_{el} and the extracted relative acoustical impedance Z_{ac}/Z_0.

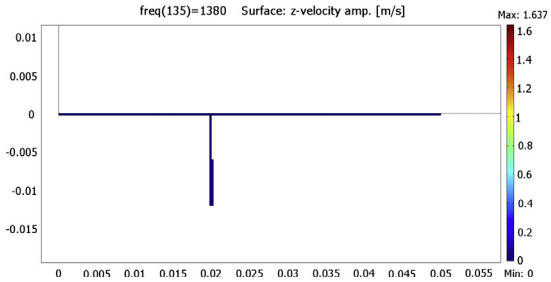

(b) Modulus of the velocity along the plate at the frequency 1380 Hz, where the electrical impedance shows a resonance.

Fig. 6. FEM results for Young modulus E_2: frequency behaviour and spatial velocity distribution at resonance.

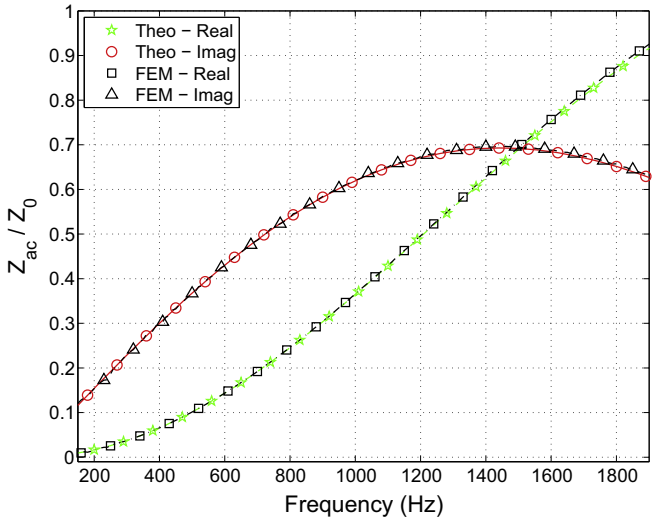

Fig. 7. Comparison between both the real (green solid line) and imaginary (red solid line) parts of the theoretical relative acoustical impedance Z_{theo} and both the real (black dotted line) and imaginary (black dashed line) parts of the extracted relative acoustical impedance Z_{ac}/Z_0. [Referenced colours are shown in the online version of this paper.] (For interpretation of the references to colour in this figure legend, the reader is referred to the web version of this article.)

Table 1
Parameters defining different speaker membrane geometries.

	Geometry I	Geometry II	Geometry III
R	5.0 cm	5.0 cm	5.0 cm
r	2.0 cm	2.0 cm	3.0 cm
H	2.1 cm	5.7 cm	3.7 cm
h	1.6 cm	5.0 cm	3.0 cm

while the acoustical absorption is only a function of the ending' s characteristics. Even if there is a loss of information, it is simpler to observe the behaviour of the absorption rather than the impedance one. In the following the evaluation of the absorption is showed using the calculated acoustical impedance.

Fig. 9 shows results for the FEM calculated acoustic absorption. Actual experimental values are reported as well as the one obtained from Eq. (5) with the three geometries defined by Table 1. While at low frequencies, under approximately 500 Hz, there is a

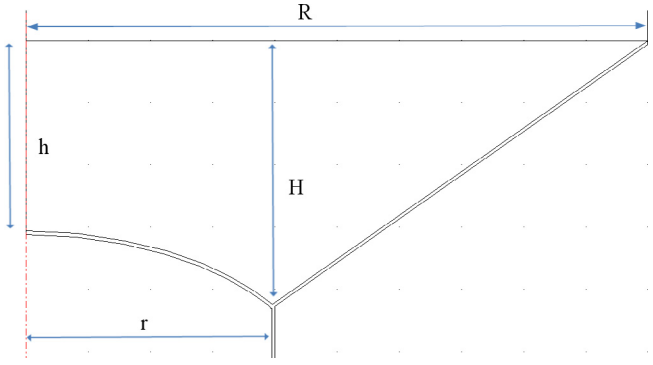

Fig. 8. Membrane shape parameters.

good agreement between the calculated and the experimental absorption, at higher values this is not true. An oscillation modulates the absorption value with an amplitude that increases with frequency, probably caused by the shape of the membrane as can be verified in the next subsection.

5.3. Acoustical absorption: effective/optimised surface method

According to the previous section, some cone shapes are investigated when subjected to different acoustical loads, obtained by two backing conditions in an impedance tube mounting. The electrical impedance is then computed by means of FEM simulation and an acoustical surface load is calculated according to Eq. (5). To simplify comparison for different materials and geometries a relative absorption index is calculated as

$$\alpha_{ratio} = \frac{\alpha_{exp} - \alpha_{FEM}}{\alpha_{exp}} \tag{10}$$

where α_{exp} is the acoustical absorption obtained from the imposed backing impedance and α_{FEM} is the one from the Z_{el} extracted acoustical impedance. A value close to zero implies that the system is accurately measuring the acoustical absorption.

The calculated impedances suffer from an oscillating behaviour. Figs. 10 and 11 present the same set of data arranged respectively by material and geometry and it can be noticed that the effect can be seen as both a function of the speaker' s geometry and of the acoustical load. From the geometric point of view, the phenomena is greatly amplified in Geometry II (the one with the steepest

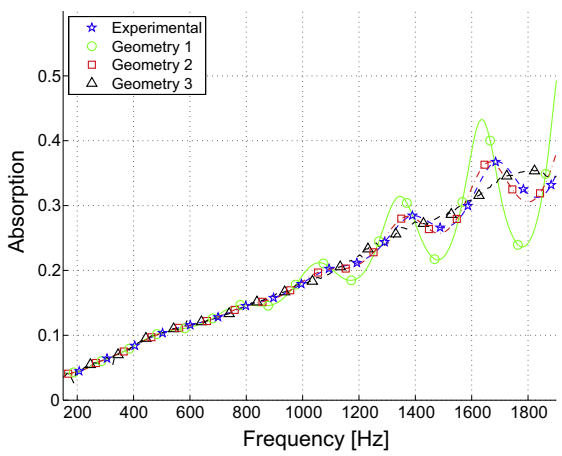

(a) Acoustical absorption α for the melamine foam.

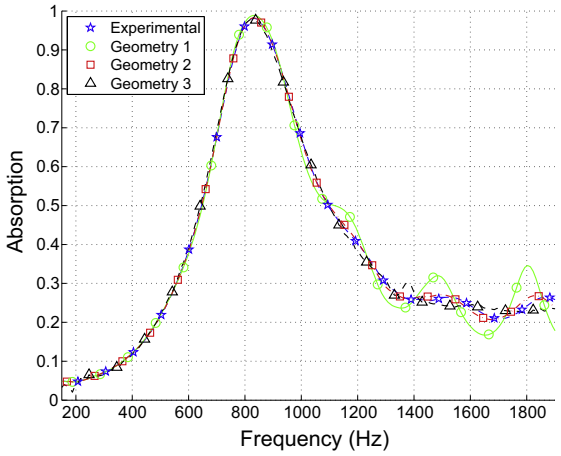

(b) Acoustical absorption α for the pavement.

Fig. 9. Each graph contains values obtained for Geometry I (blue), II (green) and III (red). [Referenced colours are shown in the online version of this paper.] (For interpretation of the references to colour in this figure legend, the reader is referred to the web version of this article.)

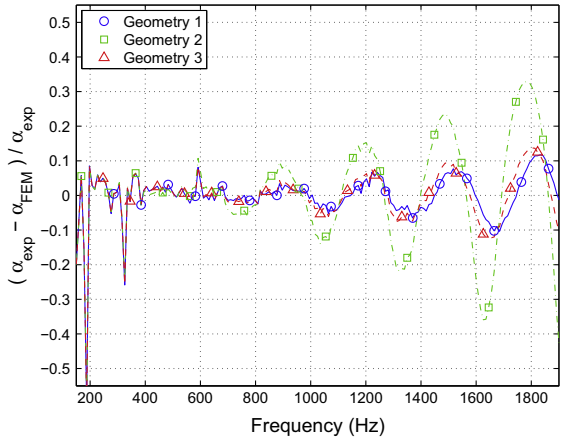

(a) Relative acoustical absorption α_{ratio} for the melamine foam.

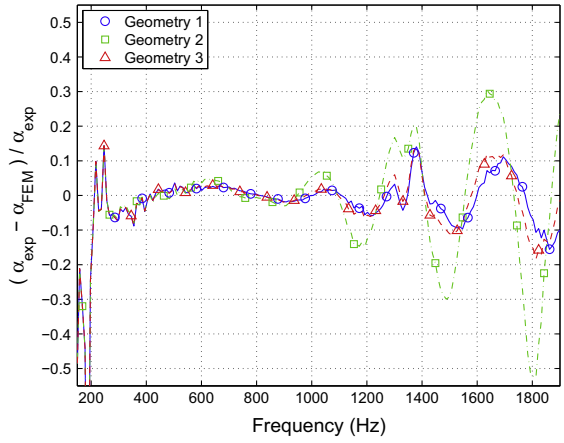

(b) Relative acoustical absorption α_{ratio} for the pavement.

Fig. 10. Each graph contains values obtained for Geometry I (blue), II (green) and III (red). [Referenced colours are shown in the online version of this paper.] (For interpretation of the references to colour in this figure legend, the reader is referred to the web version of this article.)

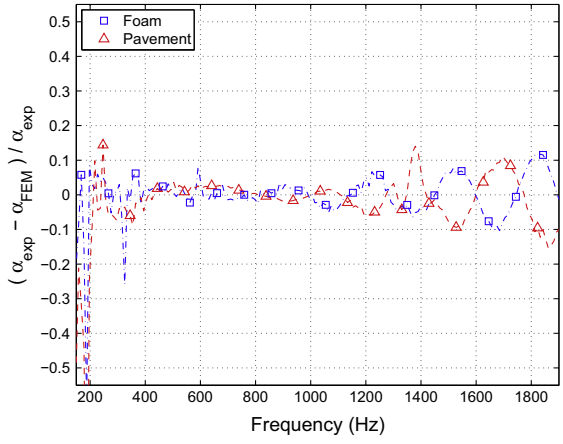

(a) Relative acoustical absorption α_{ratio} for Geometry I.

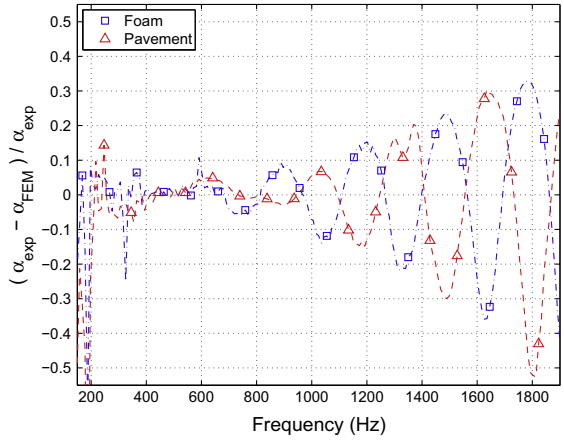

(b) Relative acoustical absorption α_{ratio} for Geometry II.

Fig. 11. Each graph contains values obtained for the melamine foam (blue) and the pavement (red). [Referenced colours are shown in the online version of this paper.] (For interpretation of the references to colour in this figure legend, the reader is referred to the web version of this article.)

lateral cone surface inclination) and the position of the peaks is dependent on the acoustical load. Finally, the effect shows a general growth according to the frequency, in fact the effect is very small in the low frequency range.

Eq. (5) does not seem able to account for this effect, however a first step towards its comprehension can be taken by observing that, while Z_m, Bl and Z_b are physical quantities derived in a lumped variables framework, A_{sp} maintains information on the actual geometry. It could be useful to introduce an optimised speaker surface A_{opt} defined as

$$A_{opt} = s_i \cdot A_{tot} \tag{11}$$

where s_i is a constant function of the geometry and the acoustic load as stated before and A_{tot} the actual speaker total membrane surface. A simple calculation is performed to evaluate s_i by minimising the difference between the experimental absorption and the one reconstructed by Eq. (5) from the simulations, having substituted the speaker surface with the optimised one. Results are presented in Table 2, where the first row is the ratio between the maximum radius surface A_0 ($r_0 = 5$ cm) and the total surface and the others are the calculated ratios for the melamine foam and the pavement.

While the optimised surface model does not explicitly take into account any dependence on the acoustical load and on frequency, the values obtained in Table 2 are clearly strongly dependent on geometry, even though they are less influenced by the considered material. In Fig. 12 the relative acoustical absorption for Geometry I and II obtained using the optimised surface is represented. It is evident how the mid-high frequency region has a better behaviour than in Fig. 11, while the lower frequencies are worsened. However it is worth noticing that a relative high value of the uncertainty in the low frequency range is less relevant than a similar relative value at high frequency, considering that absorption typically increases with the frequency. This concept is expressed for the absolute absorptions of Fig. 13: the high frequency oscillation presented in Fig. 9 is reduced, especially for the pavement.

Table 2
Ratio between the optimised and total speaker surface for the analysed geometries.

A_{opt}/A_{tot}	Geometry I	Geometry II	Geometry III
S_0	0.832	0.512	0.582
S_{Mel}	0.893	0.641	0.635
S_{Pav}	0.867	0.585	0.610

6. Discussion

In the model no hypothesis on the speaker' s mechanic impedance has been made. Eq. (5) formally does not require any particular behaviour for Z_m, with the exception of the mathematical request of a non-zero denominator. The straightforward consequence is that the speaker can be characterised for any given frequency for which the Eq. (5) is valid. On the contrary, the linear piecewise model by Ahadi and Bakhtiar gives a direct result only for frequency bands, besides imposing a limitation on the mechanical system used. However the linear piecewise model gives an explicit solution for R_m, M_m and C_m, while the more general approach model, presented in this work, can only distinguish between the real and imaginary parts of Z_m. The inductive and capacitive elements, generally functions of the frequency, cannot be clearly separated. It has to be noted that at very low frequencies the spring force factor has the main imaginary term contribution, while the mass term gets stronger with increasing frequencies. On this basis, the two models should show similar parameter values when applied in their low and high frequency limits.

Another important consideration arises from the dependence between the electric and acoustic impedances of Eq. (5) and can give some restraints on the precision needed to obtain a correct acoustical measurement. An inverse proportional relationship is established between Z_{el} and Z_{ac}. It is clear that errors affecting the evaluation of the electrical parts can have dramatic effects on the acoustical one. Even in the case of a very low electrical noise measurement it is worth to notice that the actual physical variable obtained by Z_{el} is the total acousto-mechanic impedance $Z_m + A_{sp}Z_{ac}$. The knowledge of the acoustic impedance component is actually strongly dependent on how well the mechanical one is characterised. Providing insight for this concept it results that the ratio between $A_{sp}Z_{ac}$ and Z_m behaves in two very different mounting configuration for a speaker with given mechanical parameters: an infinite baffle, whose impedance is given by Eq. (7), and a finite and closed tube. The acoustical load in this case is given by [8]

$$Z_{tube} = -iZ_c \cot(k_c L) \tag{12}$$

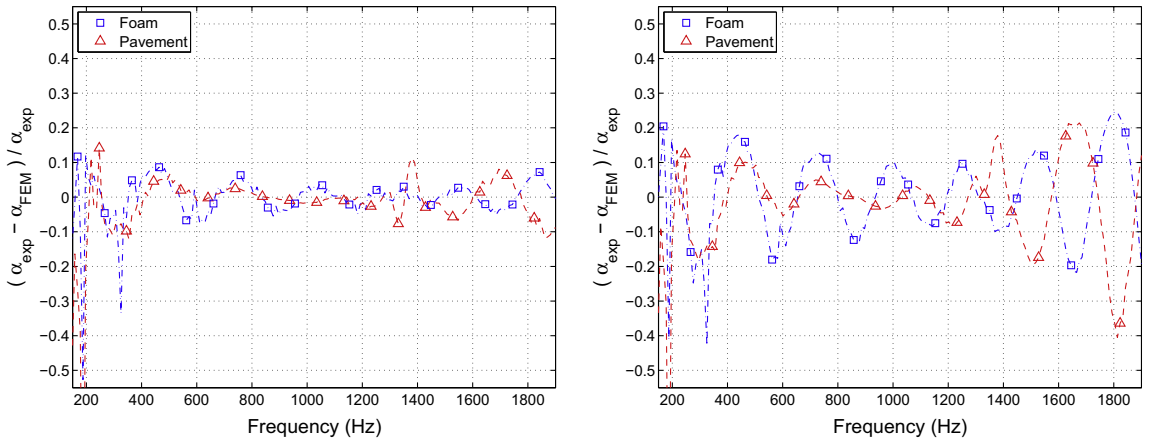

(a) Relative acoustical absorption α_{ratio} for Geometry I.

(b) Relative acoustical absorption α_{ratio} for Geometry II.

Fig. 12. Each graph contains values obtained for the melamine foam (blue) and the pavement (red). [Referenced colours are shown in the online version of this paper.] (For interpretation of the references to colour in this figure legend, the reader is referred to the web version of this article.)

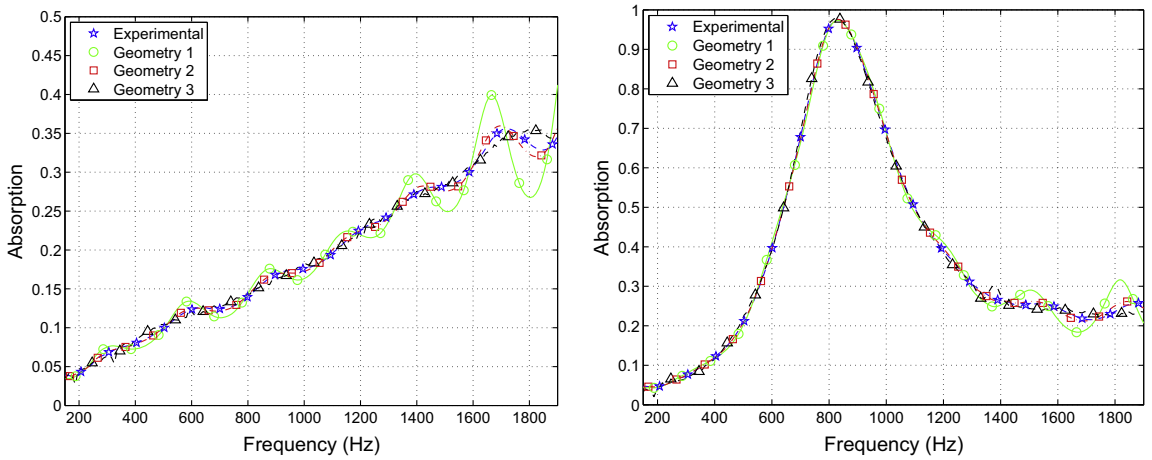

(a) Relative acoustical absorption α_{ratio} for the melamine foam.

(b) Relative acoustical absorption α_{ratio} for the pavement.

Fig. 13. Each graph contains values obtained for Geometry I (blue), II (green) and III (red). [Referenced colours are shown in the online version of this paper.] (For interpretation of the references to colour in this figure legend, the reader is referred to the web version of this article.)

Table 3
Chosen values for the numerical evaluation of the $A_{sp}\,Z_{ac}/Z_m$ ratio.

L	$5 \cdot 10^{-1}$ m
a	$5 \cdot 10^{-2}$ m
R_m	1.56 m
C_m	$1 \cdot 10^{-3}$ s^2 kg^{-1}

where the characteristic acoustic impedance Z_c and wavenumber k_c can be substituted with the exact expression for a cylindrical duct [14]. A set of reasonable values for Z_m, the duct length L and diameter $2a$ is chosen as in Table 3.

Results for the real and imaginary parts of the $A_{sp}Z_{ac}/Z_m$ ratio are shown in Fig. 14 in a frequency range from 0 to 2000 Hz. The tube longitudinal resonances cause variations from very small ratio values to very high ones in both real and imaginary part of Z_{ac}, whilst for the baffle acoustical impedance the ratio has a smoother behaviour. Both very low and very high ratio values imply a difficult evaluation of the acoustic load. For ratio lower than 10^{-2} means that $A_{sp}Z_{ac}$ is around the value of the uncertainty related to Z_m , hence the precision of the mechanic impedance knowledge sets the inferior acoustic one measurable; similarly, in case of high ratio the second term of the right side of Eq. (5) can become smaller than the precision of Z_b.

7. Conclusions

In this work the reliability of an innovative method to evaluate the acoustic impedance of a material is analysed. The tested method is based on the use of a loudspeaker as both the source of a signal and the probe. Considering the coupling between its parts as an impedance composition, the acoustic impedance can be derived from the electrical one. A FEM model was verified and used in order to evaluate the method' s critical aspects and the accuracy required for the knowledge of all various parts of the problem: the electrical and mechanical components, different speaker mounting conditions and membrane geometry. Starting from the simplest model, where the loudspeaker is a plane, the frequency range of application is determined. It has been shown that

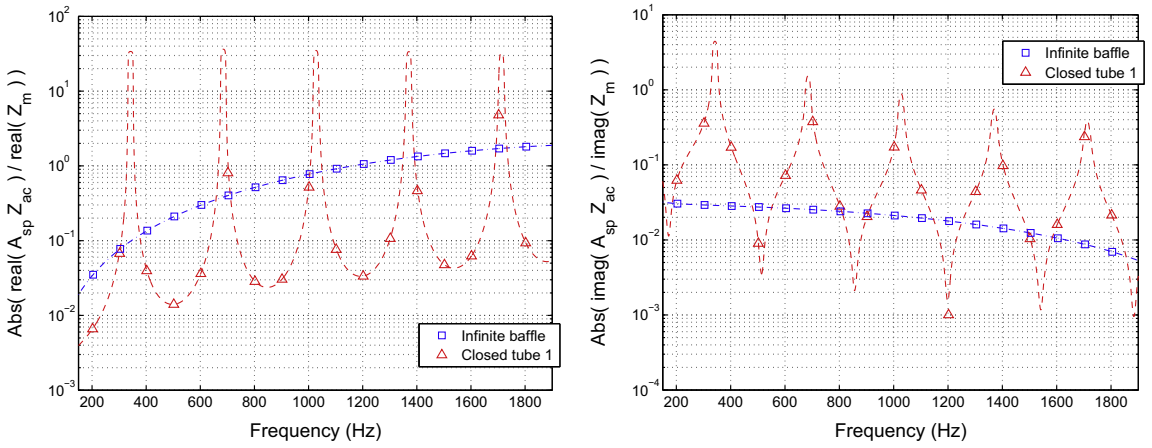

(a) Modulus of Re $(A_{sp}Z_{ac}/Z_m)$.

(b) Modulus of Im $(A_{sp}Z_{ac}/Z_m)$.

Fig. 14. Each graph contains values obtained for an infinite baffle Z_{ac} (blue) or a closed tube Z_{ac} (red). [Referenced colours are shown in the online version of this paper.] (For interpretation of the references to colour in this figure legend, the reader is referred to the web version of this article.)

when surface modes begin to appear the measure is no longer reliable. Modes affect the membrane mostly at high frequencies and the exact value at which they appear depends on both the membrane geometry and material composition. As second issue, it is investigated the required precision in the knowledge of the speaker' s mechanical, electrical and geometrical characteristics. A reference value for their relative error can be set as 10^{-4}–10^{-3} from the evaluation of an infinite baffle and a closed cylindrical duct. Finally it has been pointed out that the membrane geometry implies a frequency dependent modulation of the impedance derived acoustic absorption. The applied load can also play a role in this effect but the considered cases show that geometry has the strongest role in its explanation. An optimised membrane surface can be used, in place of the actual one, in order to partially avoid the undesired behaviour. The optimised surface can be derived by means of a FEM simulation by applying a known acoustical load on the speaker's surface and calculating the acoustic absorption from the simulated Z_{el} and it could be extended to take into account the frequency dependence. On the other side, using the FEM models it could be possible to engineer a custom shape speaker suitable to apply the method in a wider frequency range.

References

[1] Chung JY, Blaser DA. Transfer function method of measuring in-duct acoustic properties. i. Theory. J Acoust Soc Am 1980;68(3):907–13. http://dx.doi.org/10.1121/1.384778.

[2] Doutres O, Salissou Y, Atalla N, Panneton R. Evaluation of the acoustic and non-acoustic properties of sound absorbing materials using a three-microphone impedance tube. Appl Acoust 2010;71(6):506–9. http://dx.doi.org/10.1016/j.apacoust.2010.01.007. ISSN 0003-682X.

[3] ISO. 13472-2, 2011.

[4] UNI EN. 1793-5: road traffic noise reducing devices - test method for determining the acoustic performance - Part 5: Intrinsic characteristics - in situ values of sound reflection and airborne sound insulation; 2003.

[5] Anfosso FL, Garai M, Clairbois J. Une méthode européenne pour la qualification sur site des écrans antibruit. Bull. Liaison Ponts Chaussées 2000;3:89–104.

[6] Lanoye R, Vermeir G, Lauriks W, Kruse R, Mellert V. Measuring the free field acoustic impedance and absorption coefficient of sound absorbing materials with a combined particle velocity-pressure sensor. J Acoust Soc Am 2006;119(5):2826–31. http://dx.doi.org/10.1121/1.2188821.

[7] Ahadi M, Bakhtiar MS. A direct method for acoustic impedance measurement based on the measurement of electrical impedance of acoustic transmitter. Appl Acoust 2014;77:76–81. http://dx.doi.org/10.1016/j.apacoust.2013.10.008. ISSN 0003-682X.

[8] Beranek Leo L. Acoustics. New York: Woodbury; 1993.

[9] Dodd M, Klippel W, Oclee-Brown J. Voice coil impedance as a function of frequency and displacement. Audio engineering society convention, vol. 117.

[10] Klippel W. Prediction of speaker performance at high amplitudes. Audio engineering society convention, vol. 111.

[11] Marshall Leach Jr W. Loudspeaker voice-coil inductance losses: circuit models, parameter estimation, and effect on frequency response. J Audio Eng Soc 2002;50(6):442–50.

[12] Wright JR. An empirical model for loudspeaker motor impedance. Audio engineering society convention, vol. 86.

[13] Geaves GP, Henwood DJ. Finite element modelling of a loudspeaker. Part 1: Theory and validation. Audio engineering society convention, vol. 119.

[14] Allard JF, Atalla N. Propagation of sound in porous media - modelling sound absorbing materials. Wiley; 2009.